April 2024

University of Calgary

Exploring Ionospheric Behavior:

Analysis of ionosonde trends and comparison to nearby riometer activities

Name: Minoda Fernando

UCID: 30121377

Supervisor: Dr. Emma Louise Spanswick

PHYS 598

1 Abstract

The ionosphere is crucial to long distance radio communication through HF wave propagation. Two instruments used to analyze behaviors of the ionosphere are ionosondes and riometers. This thesis investigates the correlation between riometer activity at Dawson, Yukon, that is operated by the University of Calgary and the occurrence of fill values in the Gakona, Alaska ionosonde's Global Ionosphere Radio Observatory (GIRO) E/sporadic E layer data. By utilizing custom-made algorithms with Python on JupyterLab, I explored this connection and discovered a trend indicating a correlation between heightened riometer activity at Dawson and the Gakona ionosonde's ability to adequately measure the E/sporadic E layer; high riometer absorption was associated with low ionosonde measurement counts. The significance of this study lies in recognizing potential biases towards low absorption when utilizing ionosondes during high absorption events.

2 Introduction

2.1 The Ionosphere

The ionosphere is a region in the Earth's atmosphere, sitting at about 50km to over 500km [1]. It was formally defined in 1950 by a committee of the Institute of Radio Engineers as "the part of the Earth's upper atmosphere where ions and electrons are present in quantities sufficient to affect the propagation of radio waves". The varying densities of these electrically charged particles affect high frequency HF (3 – 30 MHz) propagation [2]. The variation of the ionospheric electron densities is primarily caused by photoionization [2], which is a process that ionizes atoms and molecules using a high-energy photon source – mainly the UV radiation from the Sun [3]. This results in a higher electron density during the day than at night [2].

The reflection, refraction, and absorption of HF signals depend on the density of the charged particles and the frequency of the signal. When the density is not high enough, the signals tend to pass through [8]. This occurs because when the density is lower, the critical frequency (point of maximum electron density of a certain ionospheric region) decreases. If the HF signal exceeds the critical frequency, the signal travels upward to a region where the electron density and, therefore, the critical frequency, is higher. When the HF signal traverses through these regions of varying electron densities, it undergoes refraction – similar to how light bends when travelling through glass or water. This refraction enables the HF waves to move along the curvature of the Earth, resulting in over-the-horizon communication.

The absorption of HF signals is also affected by the rate of collision of ionized particles with neutral particles [2] – adding more complexity to HF propagation in the ionosphere. This absorption can be described by the simplified version of the Appleton-Hartree equation below,

$$A = 4.6 \times 10^{-5} \int_h \frac{N_e \nu}{\nu^2 + (\omega \pm \omega_L)^2} dh$$

where A = absorption (dB), h = height (kM), N_e = electron density (m^{-3}), ν = electron-neutral collision frequency (collision frequency between ionized particles and neutral particles) (MHz), ω = angular frequency of radio wave, and ω_L = electron gyrofrequency [7]. This integral is the standard equation for ionospheric absorption and represents the cumulative effect of absorption as the height the radio wave travels (h) increases from lower altitudes to higher altitudes.

When the electron density, N_e, in increased at lower heights where the electron-neutral collision frequency, ν, is high, you observe absorption. Meanwhile, when the electron density is increased at higher altitudes where the electron-neutral collision frequency is much lower (for example, the F region), little to no absorption is observed at those altitude ranges.

Different layers of the ionosphere have their own characteristics based on electron densities. These layers were thought to be distinctly separated but are now known to overlap with each other [1]. The nomenclature was introduced by Edward V. Appleton, a pioneer in the early exploration of radio technology using the ionosphere. Namely, they are the D, E, F1, and F2 layers.

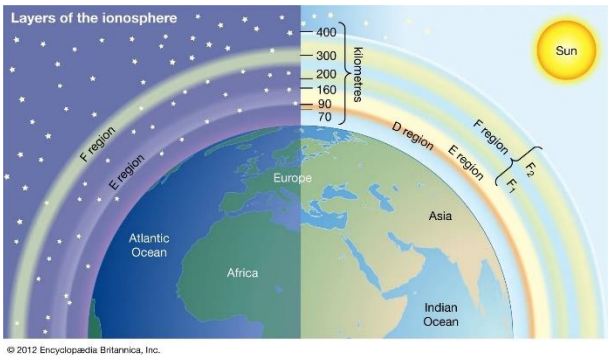

Figure 1: *Diagram of the layers of the ionosphere 1*

2.1.1 D layer

The D layer is the lowest layer sitting between 60 – 90 km [2]. The HF frequency bandwidth is too high for any reflection of signals in this layer as the electron densities are relatively low. However, the absorption levels in the D layer may be significantly high due to the presence of a high neutral density. The charged particles in this layer recombine with oxygen ions to produce neutral oxygen molecules, making the free electrons disappear [1]. During this period, HF signals pass through this layer to the E and F layers where wave reflection is better. This makes radio communication more optimal at night than day.

2.1.2 E and Sporadic E Layers

The E layer, also known as the Kennelly-Heaviside layer named after electrical engineer Arthur Kennelly and physicist Oliver Heaviside [1], is at 90 – 150km above the Earth's surface [6]. The electron density of this layer is sufficient for the reflection and refraction of HF waves, making it one of the more important layers for long distance radio communication. The density of charged particles decrease at night, however, it does not completely disappear like in the D layer.

The sporadic E layer (Es) is a thin layer that represents localized spikes in electron density within regions of the E layer [4]. It typically has a vertical thickness between 0.6 – 2km [6]. The formation of the layer is still unknown; however, it can appear during any time of day [5]. Within the GIRO database, sporadic-e layers are not distinguished from thicker "auroral e-layers", they are all grouped under sporadic-e. For this study, I use the sporadic-e measurements within the GIRO database as a general indicator of the e-region characteristics.

2.1.3 F layer

The F region, sitting at 150 – 500km [2] above the Earth's surface, is the highest layer and has the highest electron density of the ionosphere [1].

Understanding the evidently complex behaviour of the ionosphere is crucial for HF communication. Ionosondes and riometers are two important instruments that use HF radio wave propagation that give valuable insights into ionospheric behavior.

2.2 Ionosonde

An ionosonde is a radar system that sends radio waves (usually in the range of 0.1 – 20MHz) [9] upwards into the ionosphere [8]. These radio waves are reflected back to a ground receiver due to the charged particles in the ionosphere, with the reflection occurring at the height where the plasma frequency of the ionosphere matches the radio wave frequency. Parameters such as the minimum virtual height, often denoted as hE, hF, hEs corresponding to each layer, and the electron density at the reflection point can be calculated by analyzing the time it takes for reflected waves to reach back to Earth.

There is a directly proportional relationship between the radio wave frequency and electron density, represented by the equation [9] below,

$$N = 0.124 \times 10^{11} \times (f)^2$$

where N is the electron density in $[m^{-3}]$ and f is the radio wave frequency in $[MHz]$.

Figure 2 [8] illustrates the mechanism of an ionosonde. The line shown in green represents the lowest transmission frequency sent while the red represents the highest. The green is reflected back at a lower height where the electron density is lowest while the orange is reflected back at the point of maximum electron density – the critical frequency. If a radio wave's frequency is above the critical frequency, it passes through the ionosphere, as shown in red.

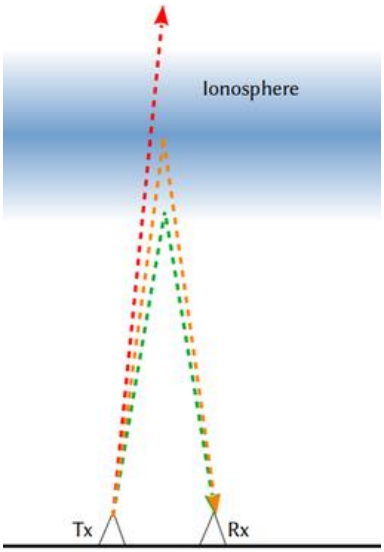

Figure 2: *Signals of different frequencies are reflected at different altitudes or escape into space. Tx = transmitter, Rx = receiver.*

2.2.1 GIRO Database

The frequencies and their corresponding altitudes determined by the ionosonde is plotted in an ionogram, from which several important ionospheric parameters can be derived.

The Global Ionosphere Radio Observatory (GIRO) is a commonly used database that provides real-time and retrospective HF ionospheric sounding data, with over 17 million ionograms and ionogram-derived records [10]. It is frequently used by scientists and researchers to analyze statistical ionospheric trends.

2.2.2 GIRO Parameters

For this project, I primarily analyzed ionogram-derived parameters from GIRO, such as the height of the sporadic E layer (hEs in km), the critical frequency of the sporadic E layer (foEs in MHz), and the critical frequency of the F2 layer (foF2 in MHz). The rationale behind selecting these parameters will be revealed in section 3 Methods.

2.3 Riometer

The relative ionospheric opacity meter, or riometer, is a passive radio antenna that measures the cosmic radio noise that can pass through the ionosphere [11]. Having different cosmic sources, such as the Milky Way, these noises are usually in a very high frequency (VHF) narrowband between 20 – 70 MHz [12], typically at about 30 MHz [11]. The free electrons in the ionosphere can absorb these cosmic noise radio waves, with the level of absorption depending on the electron density in the ionosphere. The riometer antenna detects these waves and measure their voltages that change based on the absorbed energy. This absorption is directly influenced by the electron density.

2.3.1 University of Calgary Riometer Database

The University of Calgary riometer database houses an array of riometers. As part of the Canadian Space Agency's Geospace Observatory (GO) Canada initiative, this network currently consists of 11 wide-beam riometers [13]. 18 additional riometers that are currently running would be added to this data archive and systems, while five new riometers will be deployed. The riometer used for this project is at Dawson, Yukon, shown on a map in Figure 3 [14]. The reason for choosing Dawson will be discussed below, in the 2.4 Motivation section.

Figure 3: *Location of Dawson, Yukon*

2.4 Motivation

During a project overseen by Dr. Emma Spanswick and Dr. Susan Skone it was noticed that the GIRO database for E layer parameters at the Gakona, Alaska ionosonde had a significant amount of "fill values" in the dataset, representing missing or undefined data. Fill values could arise due

to ionosonde instrument malfunctions, or due to algorithmic limitations in generating GIRO parameters. Such discrepancies in the data are not uncommon as ionosondes operate in harsh environments, like the North. However, the project team noticed a systematic nature to some of the fill values as they were also working with the Dawson riometer; when there is heightened riometer activity at Dawson, the Gakona ionosonde data produced fill values. Since riometers are not utilized as frequently as ionosondes, this has not been systematically studied before.

My project focuses on exploring this potential correlation, as well as general connections between E-layer parameters (reported by the ionosonde) and nearby riometer data. My goal is to uncover any correlations between the datasets and identify the circumstances under which these correlations occur.

2.4.1 Location

The ionosonde at Gakona, Alaska, and the riometer at Dawson, Yukon are analyzed in this study as they are nearest to each other – although separated by 349 km.

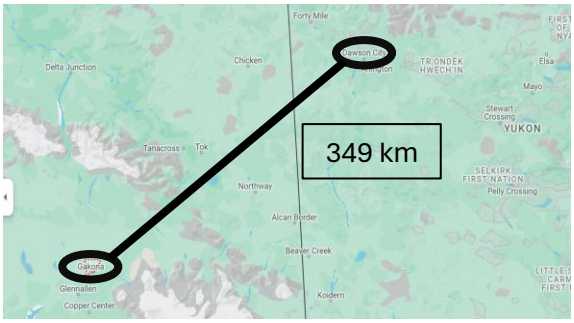

Figure 4: *Ionosonde location Gakona, AK and riometer location Dawson, YK circled on a map*

3 Methodology & Analysis

3.1 Data Acquisition and Analysis Framework

All ionosonde data used in this study is from the FastChar: Ionogram-derived data section of the Global Ionosphere Radio Observatory (GIRO) database. Within this database, I specifically use ionogram-derived data files from the Gakona, Alaska ionosonde. I also utilized the University of Calgary Riometer database for my riometer data. The riometer data files followed a specific naming convention that incorporated the respective riometer location, date, and version number.

The files I used were from the Dawson, Yukon riometer, hence the data files followed the title "`norstar_k2_rio-daws_{date}_{version}.txt`", where `k2` is denoting the level of processing, which in this case means the data was baselined and converted to decibels (dB). The version number captures any updates to the baselines, I used the latest version number to ensure that I had the most up-to-date data.

Coordinated analysis of these data required the development of a series of computer programs to read, organize, analyze, and plot the data. For this I used Python on JupyterLab, primarily using libraries such as `datetime`, `numpy`, `os`, `urllib.request`, and `calendar`. Additionally, all plotting utilized the `matplotlib.pyplot` library. The algorithms used were predominantly custom developed by me, with the help of Dr. Spanswick and her team specifically for the first read-file I needed to develop to open and read files from GIRO. In the following sections, I detail the instrument specific analysis performed to enable direct comparison of the datasets, as well as the combined analysis that supports my conclusions.

3.2 Riometer Data Analysis

The algorithms developed to open and read the necessary data files were consistently used throughout my analysis, hence, it is only appropriate to provide a brief overview of the functionality of the algorithms.

Unlike for the ionosonde read-file function (explained in 3.3.1 Ionosonde Readfile) where I saved the text files locally, the riometer read-file function, that I named '`rio_readfile`', used the `urllib.request` library to open and read the files through URL, straight from the University of Calgary riometer database. This function aims to open, read, process, and store parameters of each recorded measurement. It takes a URL parameter that points at the desired riometer data file; the

file's contents are read and decoded from an HTML to a string for further processing. This data file includes the date and time (UT), the absorption in dB, and the raw signal in volts.

The function iterates over every line in the file, skipping over comments and parsing the date and time from the non-commented lines into one datetime object. Next, to ensure the retention of only valid data, negative absorption values (and their corresponding datetime and raw signal) are discarded. The function returned a list that includes the date, time, absorption, and raw signal for each observation in each entry.

3.3 Ionosonde Data Analysis

3.3.1 Ionosonde Readfile

I retrieved the specific ionogram-derived files from GIRO and stored them as text files locally. This was because it was the first read-file algorithm I developed with Dr. Spanswick and Darren Chaddock, and local files proved to have an easier algorithm to read.

This function, that I named '`ionosonde_plotter`', aims to open, read, and store different parameters relevant to my analysis. It takes a parameter that points to the relevant text file in my local computer, which includes the datetime, foEs (critical frequency of the sporadic E layer), foE (critical frequency of the E layer), hEs (minimum virtual height of the sporadic E layer, and hE (minimum virtual height of the E layer). The function iterates over every line, skipping over commented lines, following a similar algorithm as storing each measurement in '`sanitized_data`' in the '`rio_readfile`'. This function returned '`sanitized_foEs`' and '`sanitized_hEs`' as they were the only two parameters needed for analyzing.

3.3.2 Narrowing Down the Analysis

To get an idea of the consistency of ionosonde data, I retrieved the critical frequency of the F2 layer (foF2) and the critical frequency of the sporadic E layer (foEs) from FastChar on GIRO from 2012 – 2022 following a similar algorithm as the '`ionosonde_plotter`' overviewed in 3.3.1 Ionosonde Readfile. I plotted the two parameters against time, resulting in Figure 5.

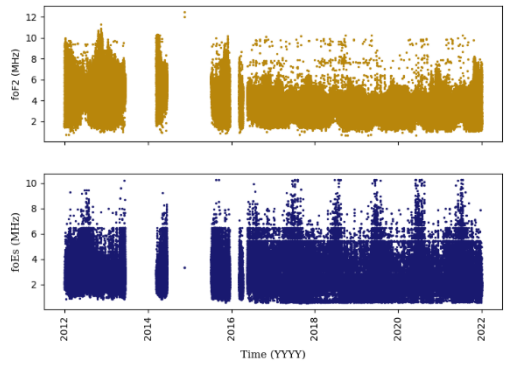

Figure 5: *Temporal evolution of the F2 Layer critical frequency, f_oF2, (top) and sporadic E layer critical frequency, f_oEs, (bottom) in MHz from January 1, 2012, to December 31, 2021*

As shown in Figure 6, the F2 layer is more susceptible to diurnal variations (fluctuations that occur during a 24-hour period – in this case, day and night – because of Earth's rotation around its axis) than the E layer. This makes the F2 layer more stable than the E layer and hence would allow for a better idea of ionosonde data consistency in the long term. I decided to narrow down my investigation to a specific timeframe of one year to simplify the data interpretation process. After examining Figure 5, I decided 2012 would be suitable as it provided consistent data across the entire 12-month period.

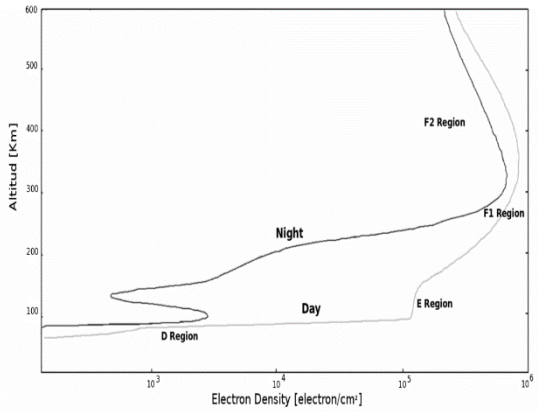

Figure 6: *Diagram of electron densities (electron/cm²) of the D, E, F1, and F2 regions against altitude for day and night.*

3.4 Synthesizing the Findings

To facilitate a focused comparison between the GIRO discrepancies and riometer absorption, I selected a specific date from 2012 where the absorption levels exceeded 3dB indicating significant levels of absorption. After careful consideration of the criteria, I opted for March 3rd, 2012.

I plotted the minimum virtual height of the Es layer (hEs), the critical frequency of the Es layer (foEs), and the riometer absorption for March 3rd, 2012, against one common time axis. This was done to validate the trend between GIRO fill values at Gakona and high riometer activity at Dawson that Dr. Spanswick and Dr. Skone observed during their project. The resulting plot is illustrated in Figure 7.

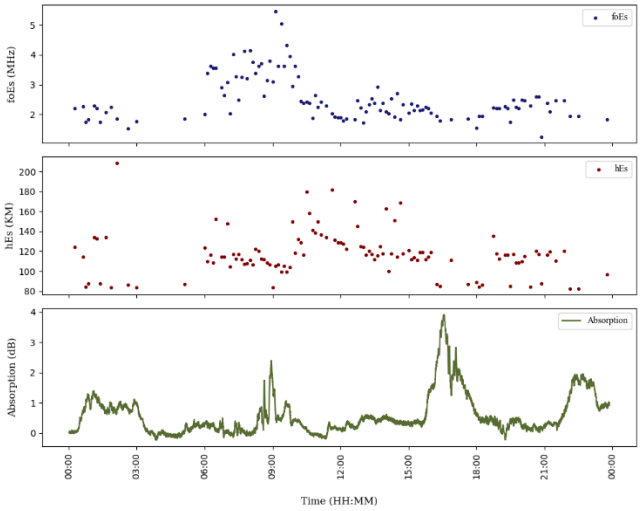

Figure 7: *[Top] Sporadic E layer critical frequency* `foEs` *in* `MHz`*, [middle] minimum virtual height of the sporadic E trace* `hEs` *in* `kM`*, and [bottom] riometer absorption in* `dB` *against common time axis for 03-03-2012*

As observed between 15:00 and 18:00 hours in this figure, there is indeed a trend where when the riometer absorption peaks, the data points in the height and critical frequencies drop.

3.5 Further Exploration

For further inspection, I selected 12 UT days from 2012 with the highest duration of time in which the riometer observed absorption above 3dB. The algorithm to execute this is as follows:

I defined a function, '`high_abs`', that takes a list as a parameter and checks the days for which absorption goes over 3dB. It counts measurements with absorptions between 3dB – 10dB and returns a 0 or 1 per day; 1 provided the count surpasses a preset threshold. The 10 dB threshold

was introduced as some absorption values significantly exceeded expected values making that data invalid for the analysis.

Next, I went over riometer files corresponding to every day of 2012, using `monthrange` from `calendar` to simplify the process. I used the '`rio_readfile`' function and passed the returned list as the parameter for the '`high_abs`' function. I stored the days which passed through '`high_abs`' in a dictionary, where the key was the date and value was the count. I then sorted the dictionary by value and selected the first 12 days from it – the 12 days with the highest count of valid riometer absorption measurements that go above 3dB.

I retrieved the ionosonde data from GIRO and riometer data from the University of Calgary riometer database for those 12 days. As for March 3rd, 2012, I plotted the minimum virtual height of the sporadic E layer (hEs), the riometer absorption for each of the days. A few of resulting plots are illustrated in Figure 8.

The same trends were observed in Figure 8 as in Figure 7, further validating that there is a potential correlation between the reduction of the Gakona ionosonde's measurement counts and high riometer activity at Dawson. However, there are instances where the ionosonde measurement counts disappear independently of high absorption levels, specifically between 01:00 – 09:00H for 03-01-2012, 06:00 – 09:00H for 07-07-2012, and 03:00 – 07: 00H for 11-07-2012 in Figure 8. This suggests that high riometer absorption is not the sole factor influencing ionosonde functionality.

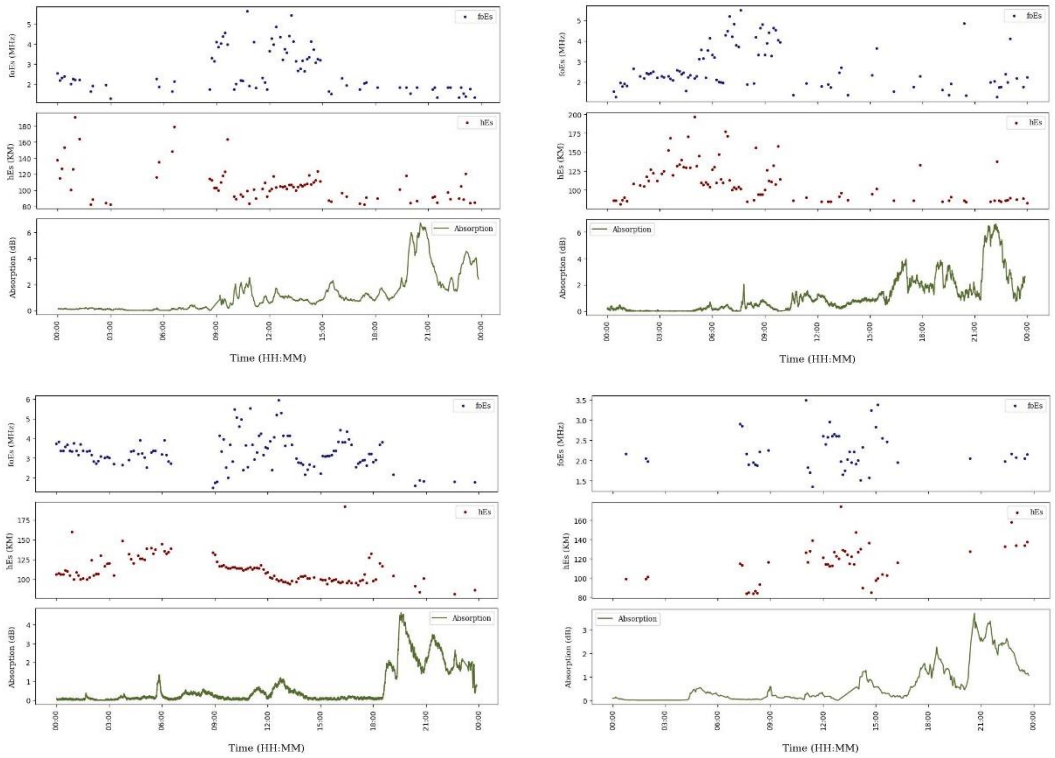

Figure 8: *Sporadic E layer critical frequency* `foEs` *in* `MHz`*, minimum virtual height of the sporadic E trace* `hEs` *in* `kM`*, and riometer absorption in* `dB` *against common time axis for [TOP LEFT] 03-01-2012, [TOP RIGHT] 04-25-2012, [BOTTOM LEFT] 07-06-2012, and [BOTTOM RIGHT] 11-07-2012*

3.6 Sporadic E Layer Height as a Function of Riometer Absorption for a 7.5 Minute Period

To confirm the consistency of the riometer data with the ionosonde data, and to confirm whether the absorption region was large enough to cover both the Gakona ionosonde and the Dawson riometer, I explored the height of the sporadic E layer (hEs) as a function of absorption for all 12 days in one plot. A plot of the critical frequency of the sporadic E layer (foEs) was made as well, however, the relationship between height and absorption is more suitable for this study. This is because changes in critical frequency correspond to changes in electron density, which needs additional information about height to place it in the context of absorption. Therefore, I will only be discussing the results of the height as a function of absorption plot in 4 Results & Discussion.

3.6.1 The Algorithm

The algorithm for this involves averaging the riometer absorption measurements for every 7.5 minutes, as the ionosonde measurements are recorded every 7.5 minutes (as opposed to every 5 seconds for the riometer). Because of the 7.5 minute gap between ionosonde records, every measurement's `datetime.minute` (which is the minute of the datetime being analyzed) is different – therefore, the fastest approach to averaging the absorption was to match each riometer measurement's minute to the corresponding ionosonde measurement's minute. When consecutive riometer measurements did not align with consecutive ionosonde measurements, the riometer measurements' absorption values were accumulated to be averaged. When a match occured, the absorptions were averaged and added to a list. The list includes the datetime of the ionosonde measurement, the riometer average, and the height from the ionosonde measurement.

The resulting plot is illustrated in Figure 9 and discussed in section 4 Results & Discussion.

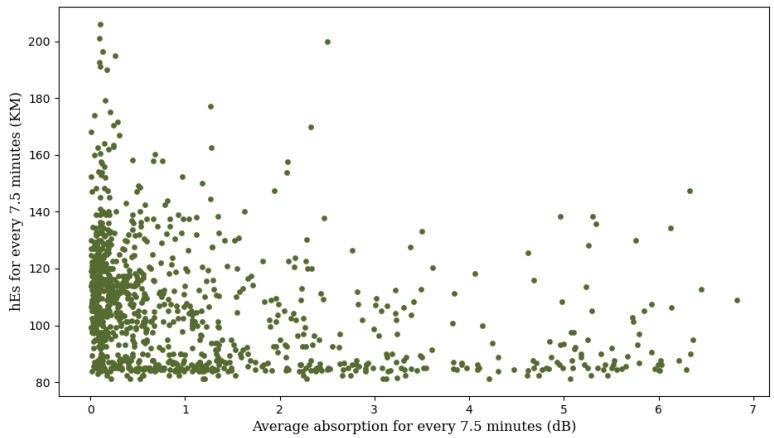

Figure 9: *Virtual height of the sporadic E layer,* `hEs (KM)` *as a function of average absorption (dB) for a 7.5-minute period for 12 UT days in 2012*

3.7 Number of hEs Points Recorded Per Hour as a Function of Hourly Average Absorption

In order to quantify the drop in density of data points in the hEs as a function of absorption, I calculated the number of recorded hEs measurements per hour as a function of hourly average riometer absorption for all 12 days in one plot. The goal of this was to help determine a statistically significant drop, if any, in the ionosonde measurement count as riometer absorption increases.

3.7.1 Usage of Default Dictionaries in the Algorithm

For this algorithm, I began using default dictionaries in the Python `collections` module. Default dictionaries have a similar functionality to dictionaries, where there is a key-value pair in which the key must be unique and immutable [15]. However, default dictionaries never raise a KeyError; instead, they provide a default value for keys that do not exist.

This significantly reduced the programming time as I did not have to keep track of multiple lists where there were fill values at different datetimes.

The default dictionary's key was the date and hour, helping organize the temporal data. For example, `'2012-01-23:22'` denotes the 22nd hour of January 23, 2012. Meanwhile, the structure of the default dictionary's value resembled this: `{'hour': -1, 'pph_hEs': 0, 'pph_foEs': 0, 'avg_absp': -1, 'peak_absp': -1}`, where `'hour'` is the hour of the day of the measurement, `'pph_hEs'` is the number of hEs points for the hour, `'pph_foEs'` is the number of foEs points for the hour, `'avg_absp'` is the average absorption for the hour, and `'peak_absp'` is the peak absorption value of that hour. The values that are in front of these parameters in the structure (`-1, 0, 0, -1, -1`, respectively) denote the default values the dictionary takes in the case that no measurement of the parameter exists. For instance, say, the average absorption is 0.53, the peak absorption is 0.85, but there were no hEs or foEs points for

March 3rd, 2012, for 3:00H. The default dictionary would store the parameters for hour 3:00 of March 3rd as: `{'2012-03-03:3': {'hour': 3, 'pph_hEs': 0, 'pph_foEs': 0, 'avg_absp': 0.536625, 'peak_absp': 0.851}`

3.7.2 Plotting Algorithm

For plotting the hEs points per hour as a function of average absorption, I focused solely on entries of the dictionary where the average absorption was not defaulted to -1, meaning I only analyzed hours of days with a riometer measurement recorded. My analysis is focused on the absent or low ionosonde measurement counts (`'pph_hEs'`) as absorption increases, therefore, absent absorptions could be ignored with no effect to the study. The resulting plot is illustrated below, in Figure 10, and discussed in section 4 Results & Discussion.

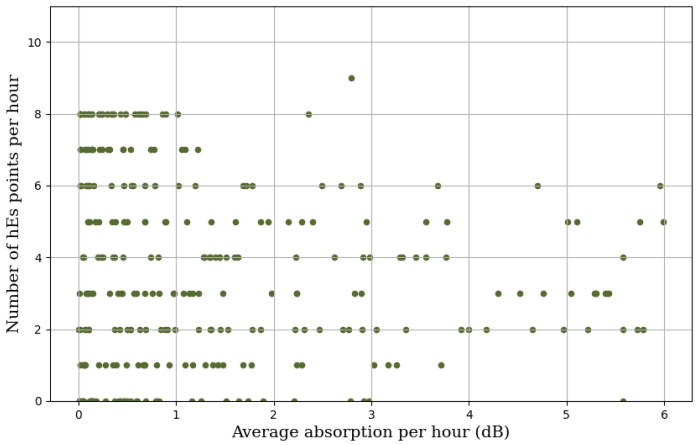

Figure 10: *The number of* `hEs` *(virtual height of the sporadic E layer) points per hour as a function of hourly average absorption* (`dB`) *for 12 UT days in 2012*

3.8 Probability of Ionosonde Functionality as a Function of Riometer Absorption

From the resulting plot Figure 10, we can further quantify the functionality of the ionosonde data products by asking the question *how does the number of data points available change with absorption?* This

provides a metric for how well the ionosonde is working and producing the hEs data product, relative to observations made by the riometer.

To accomplish this, I followed a simple algorithm where I separated the count of hEs values per hour for every absorption threshold (meaning, absorptions between 0 – 1 dB, 1 – 2 dB, till 5 – 6 dB). I introduced a data point threshold of 7. Then, I used `numpy` arrays and calculated the probability of having at least 7 data points by summing the data points greater than or equal to 7 and dividing by the size of that specific absorption threshold array.

The resulting plot is shown below, in Figure 11, and discussed in section 4 Results & Discussion.

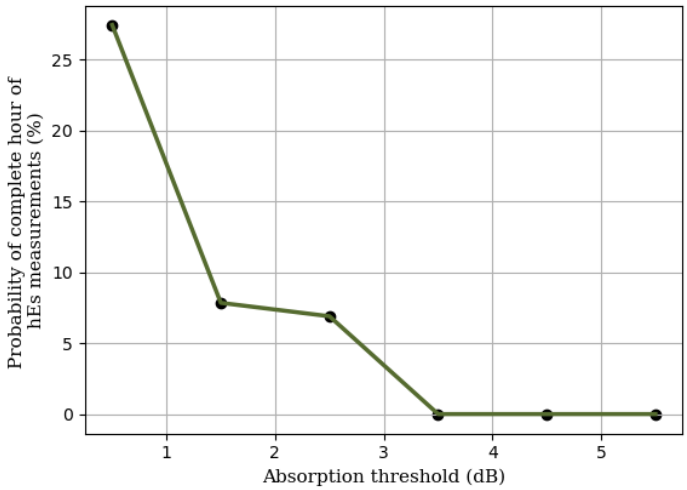

Figure 11: *The probability of a complete hour of `hEs` measurements from the Gakona ionosonde as a percentage against hourly absorption threshold (`dB`) of the Dawson riometer*

4 Results & Discussion

In this section, I will present and analyze the findings obtained from my project. First, I will discuss the results from section 3.6 Sporadic E Layer Height as a Function of Riometer Absorption for a 7.5 Minute Period. Then, I will combine the results of the two sections, 3.7 Number of hEs Points

Recorded Per Hour as a Function of Hourly Average Absorption and 3.8 Probability of Ionosonde Functionality as a Function of Riometer Absorption and discuss.

4.1 Es Layer Height as a Function of Absorption

As shown in Figure 9, the spread of heights of the Es layer decreases as absorption increases. Most of the height of the Es layer between riometer absorptions of 3 dB and 6 dB is confined to within an 80 – 100 km altitude range.

To understand this, we must refer to the ionospheric density profile and the Appleton-Hartree equation from section 2.1 Ionosphere.

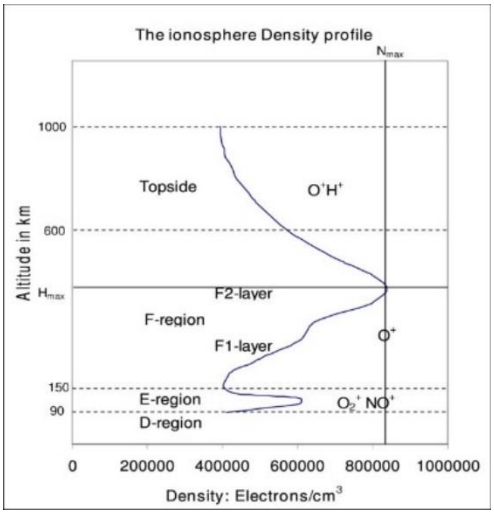

Figure 12: *Ionospheric density (electron/cm²) profile as a function of altitude (kM) for the D, E, and F regions of the ionosphere*

First, examining the altitude-dependent electron density diagram shown in Figure 12 [16], we observe the "bump" of the electron density profile of the E region.

Upon shifting the E region "bump" to a lower altitude range between 80 – 100 km, as depicted in green in Figure 13, we see an overlap of the E region with the D layer. The electron-neutral collision frequency trend in Figure 13, drawn in red based on nominal profiles, shows that the frequency at the 80 – 100 km range is much higher and increases more rapidly than at the 90 – 150 km range where the E region lay previously. The electron-collision frequency escalates from about

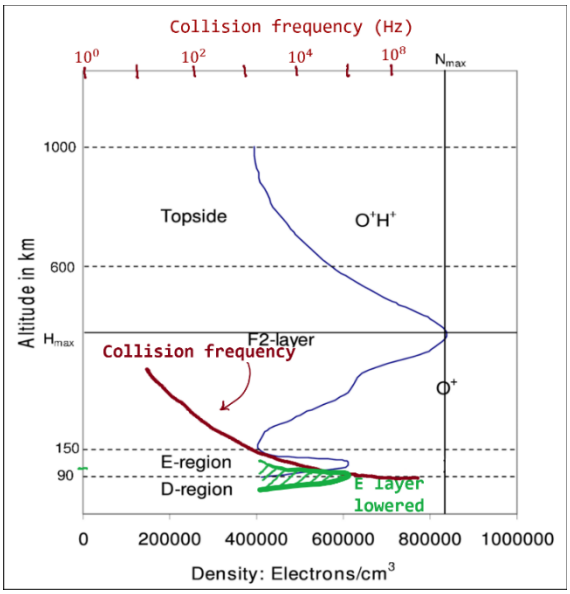

a 1000 Hz to 10,000,000 Hz as the altitude decreases from 100 km to 80 km.

The Appleton-Hartree equation for absorption [7] mentioned previously can be used to examine the underlying physics to this.

$$A = 4.6 \times 10^{-5} \int_h \frac{N_e \nu}{\nu^2 + (\omega \pm \omega_L)^2} dh$$

According to this equation, and as discussed previously, high absorption levels are observed when the density, N_e, gets to lower altitudes where electron-neutral collision frequency, ν, is higher. This is consistent with Figure 9 where a large proportion of the heights recorded at higher absorptions (3 – 6 dB) is at lower altitudes (80 – 100 km).

The overlap of the D and E layers at higher absorptions suggest that the absorption region is sufficiently large and can cover both the Gakona ionosonde and the Dawson riometer, indicating a potential correlation between the two instruments during high absorption events.

4.2 Gakona Ionosonde Functionality as a Function of Dawson Riometer Absorption

Examining Figure 10, we observe that the number of hEs points recorded per hour decreases with increasing riometer absorption. As discussed above, if we postulate 7 or more data points as an indication for the ionosonde functioning properly, we observe that after approximately 1.5 dB, there is a notable decrease in the number of hEs points available from the GIRO database.

As described in section 3.8 Probability of Ionosonde Functionality as a Function of Riometer Absorption, I estimate the performance of the ionosonde by deriving the hourly probability of a complete set of hEs measurements (as a function of riometer absorption) shown in Figure 11. This plot clearly indicates a trend, previously hinted at in plots from Figure 9 and Figure 10, whereby the ionosonde appears to function "less well" during times of high riometer absorption.

5 Conclusion

I have identified a correlation between high riometer activity at Dawson and the ability of the Gakona ionosonde to measure the E layer. This suggests that heightened riometer absorption values coincide with a lack of measurements from the ionosonde.

Some sources of error for this study include spatial variability due to the distance between observation sites, which could potentially result in incomplete data coverage due to the absorption regions not being large enough to cover both Gakona and Dawson. Additionally, instrumentation malfunctions with the ionosonde and riometer introduces inconsistencies in the recorded data. Factors such as wildlife damaging the ionosonde, and the presence of HF transmitters near riometers introducing background noises, contribute to these malfunctions. Taking these sources of error into account, and as seen in figures above, it's important to recognize that although there is a correlation between high riometer activity and low ionosonde measurement count, high frequency absorption is not the sole determinant of the Gakona ionosonde's ability to adequately measure the E layer.

This study underscores the importance of recognizing potential biases towards low absorption measurements when utilizing ionosondes during periods characterized by high absorption activity.

Bibliography

[1] McElroy, M. B. (2023), Ionosphere and magnetosphere, Encyclopædia Britannica. Available from: https://www.britannica.com/science/ionosphere-and-magnetosphere (Accessed 1 November 2023)

[2] Cameron, T. G. et al. (2021), Characterization of high latitude radio wave propagation over Canada, *Journal of Atmospheric and Solar-Terrestrial Physics*. Available from: https://www.sciencedirect.com/science/article/abs/pii/S1364682621001231 (Accessed 2 April 2024)

[3] Nishimura, Y., O. Verkhoglyadova, Y. Deng, and S.-R. Zhang (2021), Density, irregularity, and instability, *Cross-Scale Coupling and Energy Transfer in the Magnetosphere-Ionosphere-Thermosphere System*. Available from: https://www.sciencedirect.com/science/article/abs/pii/B9780128213667000019 (Accessed 2 April 2024)

[4] Arras, C., L. C. A. Resende, A. Kepkar, G. Senevirathna, and J. Wickert (2022), Sporadic E layer characteristics at equatorial latitudes as observed by GNSS radio occultation measurements - earth, planets and space, *SpringerOpen*. Available from: https://earth-planets-space.springeropen.com/articles/10.1186/s40623-022-01718-y (Accessed 9 April 2024)

[5] Niu, J., and H. Fang (2022), An Empirical Model of the Sporadic E Layer Intensity Based on COSMIC Radio Occultation Observations, *AGU Publications*. Available from: https://agupubs.onlinelibrary.wiley.com/doi/full/10.1029/2022SW003280 (Accessed 9 April 2024)

[6] Emery, W., and A. Camps (2017), Sporadic E layer - Microwave Radiometry, *Sporadic E Layer - an overview | ScienceDirect Topics*. Available from: https://www.sciencedirect.com/topics/earth-and-planetary-sciences/sporadic-e-layer (Accessed 9 April 2024)

[7] Ranta, H., and A. Ranta (2003), Riometer measurements of Ionospheric Radio Wave Absorption, *Science Direct*. Available from: https://www.sciencedirect.com/science/article/abs/pii/0021916978900314 (Accessed 9 April 2024)

[8] Anon (n.d.), Ionosonde, *PITHIA*. Available from: https://pithia-nrf.eu/activities-results/outreach/space-weather-research-instruments/ionosonde (Accessed 3 November 2023)

[9] Radicella, S. M., and Y. O. Migoya-Orué (2021), Ionosondes - GNSS-derived data for the study of the ionosphere, *Ionosondes - an overview | ScienceDirect Topics*. Available from: https://www.sciencedirect.com/topics/earth-and-planetary-sciences/ionosondes (Accessed 9 April 2024)

[10] Anon (n.d.), Global Ionospheric Radio Observatory (GIRO), FastChar Digital Ionogram Database. Available from: https://giro.uml.edu/

[11] R.A.D. Fiori, and D.W. Danskin (2016), Examination of the relationship between riometer-derived absorption and the integral proton flux in the context of modeling polar cap absorption, *AGU Publications* from: https://agupubs.onlinelibrary.wiley.com/doi/full/10.1002/2016SW001461

[12] Marshall, R. A., and C. M. Cully (2020), Atmospheric effects and signatures of high-energy electron precipitation, *Riometers - an overview | ScienceDirect Topics*. Available from: https://www.sciencedirect.com/topics/earth-and-planetary-sciences/riometers (Accessed 9 April 2024)

[13] Anon (2023), Aurora: Projects: GO-rio, *University of Calgary*. Available from: https://www.ucalgary.ca/aurora/projects/rio (Accessed 9 April 2024)

[14] Anon (2024), Dawson, *Encyclopædia Britannica*. Available from: https://www.britannica.com/place/Dawson-Yukon (Accessed 9 April 2024)

[15] GfG (2023), Defaultdict in python, *GeeksforGeeks*. Available from: https://www.geeksforgeeks.org/defaultdict-in-python/ (Accessed 9 April 2024)

[16] Sibanda, P. (2014), Particle Precipitation Effects on the South African Ionosphere, *Research Gate*, 18. Available from: https://www.researchgate.net/publication/29806954_Particle_precipitation_effects_on_the_South_African_ionosphere#fullTextFileContent (Accessed 2 April 2024)

Appendix

GitHub link to my work with Python: https://github.com/minodafernando/PHYS-598